On the Homoclinic Tangles of Henri Poincaré

Qiudong Wang

1. Introduction

It is well acknowledged that Poincaré's discovery of homoclinic tangles marked the beginning of the modern chaos theory. Poincaré studied the solution of differential equations in the form of

$$\frac{dx}{dt} = f(x) + \varepsilon g(x,t) \tag{1.1}$$

where $x \in \mathbb{R}^2$ is the phase variable, $g(x,t)$ is time-periodic, and ε is a small parameter. He observed that, under the assumption that the unperturbed equation

$$\frac{dx}{dt} = f(x) \tag{1.2}$$

has a saddle fixed point x_0 with a homoclinic solution $x(t)$ so that $\lim_{t\to\pm\infty} x(t) = x_0$, time-periodic perturbation $\varepsilon g(x,t)$ induces exceedingly complicated dynamic structures in the vicinity of the unperturbed homoclinic solution $x(t)$, which he named as *homoclinic tangles*.

In this paper, we introduce to the reader a recent theory on the dynamics of homoclinic tangles of equation (1.1). Our objective is to understand and to describe the dynamic structure of the invariant set of solutions of equation (1.1) in the vicinity of the unperturbed homoclinic solution $x(t)$. Since equation (1.1) is with a small parameter ε, this objective is then divided into two: the first is to describe the dynamic structure of a homoclinic tangle for a given value of ε and the second is to tell in what way the tangles of different ε fits together.

We assume x_0 is a *dissipative* saddle. This is to say that we assume the negative eigenvalue of the Jacobian matrix $Df(x_0)$ is larger than the positive eigenvalue in magnitude. We will illustrate that Smale's horseshoe, SRB measure of Benedick-Carleson and Young, and Newhouse sinks are all participating elements inside of the homoclinic tangles of equation (1.1). It has also turned out that homoclinic tangles of different dynamic structures are organized, asymptotically, in an infinitely refined pattern defined on parameter intervals of a fixed length of $\ln \varepsilon$, and this asymptotic pattern is repeated indefinitely as $\varepsilon \to 0$.

This exposition is divided into two parts. Sections 2-6 are the first part and Sections 7-9 are the second part. In Sections 2 and 3, we give a rather detailed recounting on the circumstances and events that led to the discovery of homoclinic tangles to recall the prominent role homoclinic tangles of equation (1.1) played in this mathematical venture in history[1]. In Sections 4-6, we introduce to the reader, one by one, the participating dynamic objects inside of the homoclinic tangles of equation (1.1). Section 4 is on Smale Houseshoe, Section 5 is on the SRB measures of Benedick-Carleson and Young, and Section 6 is on the Newhouse theory. Since the discoveries of these participating dynamic objects were stretched over a long period of time and each of these discoveries has been an event of substantial influence on its own in the development of the modern theory of dynamical

[1] We note that Poincaré did not consider the case x_0 is dissipative. In his study all that mattered were conservative mechanic systems.

systems, this part also serves as a review on history. The scope of this review, however, is restricted on the dynamic objects contained in the homoclinic tangles of equation (1.1). Our purpose is to introduce a recent theory on this specific class of homoclinic tangles and to put this theory in historic perspective for the reader, not to make a complete survey on the study of homoclinic tangles as a generic dynamic object.

The result of our theory is presented in Sections 7-9, where we put the various components introduced in the first part together to present an overview. The roles each of these dynamic objects plays as a participating part of the homoclinic tangle of equation (1.1) are made clear in Sections 7 and 8. In Section 9 we present a systematic numerical method based the theory presented in Sections 7 and 8 for numerical simulations in the surroundings of the unperturbed homoclinic solutions of equation (1.1).

This paper is not written exclusively for experts on the subject matter. It is also for people with a generic interest in modern chaos theory and its applications to the study of ordinary differential equations. A generic reader should be able to breeze through Sections 2-4 because of his/her previous exposure to the subject matter. However, it is unseemly that a non-expert would have been exposed to all that is presented in Sections 5 and 6. Substantial efforts are put forth in the writing of these two sections to make the main conclusions of certain sophisticated dynamics theories accessible to non-experts.

2. King Oscar II's prize on the N-body problem

Our story started with a prize established by King Oscar II of Sweden and Norway in 1888 for solving the Newtonian N-body problem. At the time it was a common practice to set up a prized competition to promote a new scientific journal. Seeking to promote the newly launched *Acta Mathematica*, Gösta Mittag-Leffler, his Majesty's science adviser, prompted the King to set up this royal competition. The prize committee was comprised of Charles Hermite, Gösta Mittag-Leffler and Karl Weierstrass. Since the committee could not use a vague term such as "solving the N-body problem" to define the main objective of this competition, it first had to decide in precise terms a way in which the N-body problem could be deemed as a resolved mathematical problem. This task was delegated to Weierstrass, and the formulation he came up with, formally introduced in the official announcement for the prize in *Acta Mathematica*, vol. 7, of 1885-1886, was as follows:

Given a system of arbitrarily many mass points that attract each other according to Newton's law, under the assumption that no two points ever collide, try to find a representation of the coordinates of each point as a series in a variable that is some known function of time and for all of whose values the series converges uniformly.

The proposed power series solutions were constructed by Karl Sundman twenty six years later for the 3-body problem ([38], [33])), and by myself at a much later time for all N ([40]). In both cases, however, the power series constructed converge so slowly that they were practically useless. My construction, fulfilling all that was required in that official announcement, is *tricky* but surprisingly *simple*. A question with a tricky, simple, and useless answer is not the kind the prize committee ought to have asked. This, therefore, was their first mathematical mistake.

When the problem was first proposed, Henri Poincar, the greatest mathematical genius of the time, began working on it. In a letter addressed to Mittag-Leffler, Poincaré claimed to have proven a stability result for the restricted three-body problem. He wrote ([14], page 44)

In this particular case, I have found a rigorous proof of stability and a method of placing precise limits on the elements of the third body... I now hope that I will be able to attack the general case and ... if not completely resolve the problem (of this I have little hope), then at least found sufficiently complete results to send into the competition.

Soon after, Poincar submitted his paper, and was awarded the prize. His paper was dually refereed by Mittag-Leffler and Weierstrass, and the latter asserted in his report to the former that ([14], page 44)

I have no difficulty in declaring that the memoir in question deserves the prize. You may tell your Sovereign that this work can not, in truth, be considered as supplying a complete solution to the question we proposed, but it is nevertheless of such importance that its publication will open a new era in the history of celestial mechanics. His Majesty's goal in opening the contest can therefore be considered attained.

It was, however, soon realized that Poincaré's prize winning paper contained a fatal mathematical error, and the stability result he claimed to Mittag-Leffler was wrong. It appeared that Poincar himself spotted the fatal error when answering certain questions raised by Edvard Phragman, who was copy editing Poincaré's paper to be published by Acta Mathematica.

The prevailing opinion in later times concerning the mistake and the award was perhaps reflected best in the following passage, written by F. R. Moulton in 1912 ([24]).

While the error was unfortunate, there is not the slightest doubt that in spite of it, and even had it been known at the time, the prize was correctly bestowed. If all the parts affected by the error are omitted, the memoir still remains one whose equal in originality, in results secured, and in extent of valuable field opened, is difficult to find elsewhere. There are but few men, even of high reputation, who have produced more in their whole lives that was really new and valuable than that which was correct in the original investigation submitted by Poincaré.

However, mistakes were mistakes, and the mistake made by the committee to award a grand prize to a paper with a fatal mathematical error was an unpleasant reality with which Mittag-Leffler had to reckon. When the mistake was uncovered, Poincaré's original submission was already in print. Mittag-Leffler decided to make a recall, and ordered all copies with Poincaré's original paper to be physically destroyed. Poincaré paid twice as much as the prize money he received to cover the cost of this recall. At this point, Mittag-Leffler was in a real difficult situation. He needed to maintain a high scientific and ethic standard and at the same time, control a potential fallout that was at the very least a great embarrassment. After all, there were others who had put forth great effort in participating in this competition and were arguing that their work was more deserving to win the prize.

In trying to reckon with the *mathematical* consequences of his mistake, Poincaré discovered the homoclinic tangle therefore gave birth to the chaos theory, a mathematical theory of great influence in later times. Poincaré's paper, published by *Acta Mathematica* ([29]) after the recall, is a true masterpiece and is that history has proven to equal all that was asserted in Weierstrass's report.

3. Discovery of Homoclinic tangles

Mittag-Leffler's order to destroy all recalled copies of Poinacré's original submission was not thoroughly carried out. At least one copy was uncovered one hundred years later by Richard McGehee, whose research was primarily on the three-body problem.[2]

To understand the error in Poincaré's paper and the mathematical discovery that followed, we need to start with the geometric point of view Poincaré introduced in the study of ordinary differential equations ([28]). Let $x = (x_1, \cdots, x_n)$ be an n-vector and t be the time. Let

$$\frac{dx}{dt} = f(x) \tag{3.1}$$

be a set of ordinary differential equations for x. Before the time of Poincaré, mathematicians had tried to *solve* equation (3.1) by deriving an *explicit* formula of solutions of x in t. Since solutions in closed form are in general not attainable, power series were used as a substitute. However, power series only converge on finite time interval, and the size of the convergence interval varies depending on the location of the solution. Weierstrass's formulation of the King's prize problem was a reflection of the mainstream perception of his time. He equated the task of solving the N-body problem to the task of finding a power series solution that converges for all time.

Poincaré's geometric point of view, which is quite simple, is to view an n-vector as a point in $\mathbb{R}^n$ which he called the *phase space*, and to view solutions as a collection of non-intersecting curves in this phase space. He pointed out that, as a mathematical problem, the questions we should ask in the study of equation (3.1) are (a) what kind of solution curves are allowed by equation (3.1), and (b) in what way all solution curves fit together.

The ordinary differential equation Poincaré was toiling on for the King's prize was not exactly like equation (3.1). It is in the form of

$$\frac{dx}{dt} = f(x) + \varepsilon g(x, t) \tag{3.2}$$

where ε is a small parameter and $g(x, t)$ is a function that is periodic in t of, say period T. One good thing about the restricted 3-body problem, which was the subject of Poincaré's investigation, is that the equation for $\varepsilon = 0$ is completely solvable, so he knew everything about the solution curves and the way they fit together. In particular, he knew that there is an equilibrium solution, to which a family of solutions asymptotically approach in both the backward and the forward time. Poincaré called these solutions *homoclinic*. Homoclinic solutions form a nice invariant surface in phase space. Now the question is what happens to this nice invariant surface when ε is not zero? Here Poincaré mistakenly argued that this invariant surface remained intact.

Poincaré explained the situation later by using equations with a two dimensional phase space ([30]). To study the solutions of (3.2), Poincaré explained, is the same as to study the iterations of a one parameter family of maps that is defined by the solutions of equation (3.2). Let $x(t, x_0, \varepsilon)$ be the solution of (3.2) satisfying $x(0, x_0, \varepsilon) = x_0$, the *time-$T$ map* Poincaré iterated is $F_\varepsilon : x_0 \to x(T, x_0, \varepsilon)$. See Figure 1. For equation (3.2), F_ε is a one parameter family of maps and ε is the parameter.

[2]McGehee introduced a new set of variables to study the solutions of the N-body problem near triple collision ([20]). His new variables were used to construct solutions of non-collision singularity for the N-body problem [47]. My construction of the aforementioned power series solution was also based on a revised version of McGehee's coordinates.

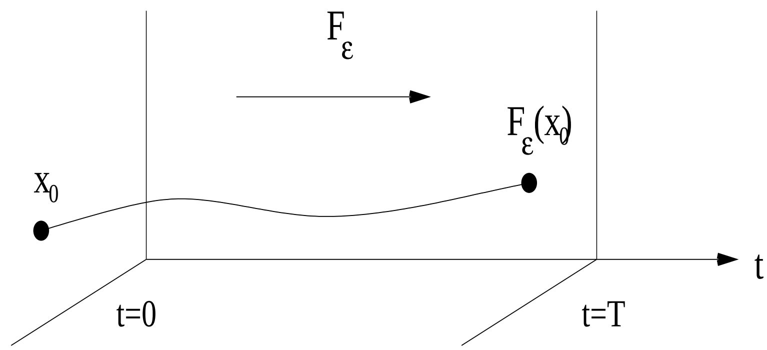

Figure 1. The time-T map

Let ℓ_0 be the trajectories of homoclinic solutions of the unperturbed equation ($\varepsilon = 0$) in phase space. Under the iterations of F_0, the time-T map for the unperturbed equation, ℓ_0 is an *invariant loop*. This is to say that $F_0(\ell_0) = \ell_0$. See Figure 2(a). Small perturbation, unfortunately, would break this loop into two non-tangentially intersecting curves, one of which we denote as ℓ_ε^s, and the other we denote as ℓ_ε^u. We have $F_\varepsilon(\ell_\varepsilon^s) \subset \ell_\varepsilon^s$, and $F_\varepsilon^{-1}(\ell_\varepsilon^u) \subset \ell_\varepsilon^u$. We name ℓ_ε^s as the stable manifold and ℓ_ε^u as the unstable manifold of the saddle fixed point of F_ε. See Figure 2(b).

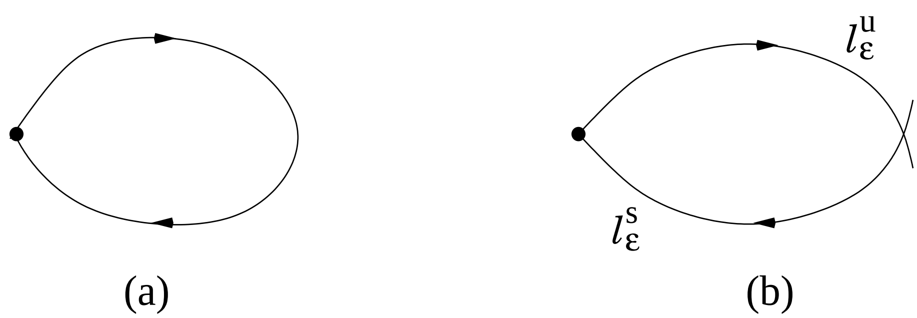

Figure 2. Non-tangential intersection of stable and unstable manifold

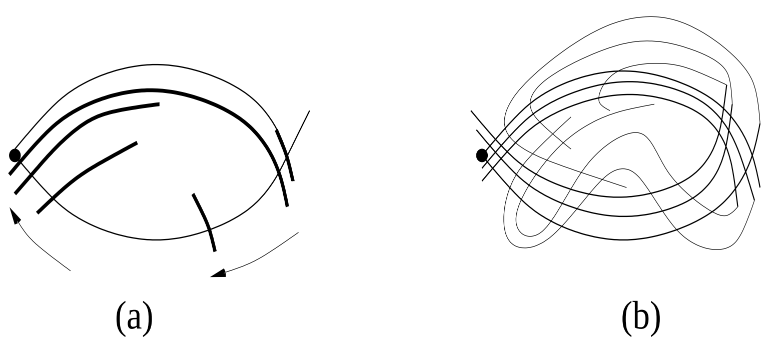

Figure 3. Formation of homoclinic tangle

Let p_0 be the point of intersection in Figure 2(b). It is on the stable manifold so $p_n = F_\varepsilon^n(p_0)$ would approach the saddle fixed point as $n \to +\infty$. It is also on the unstable manifold so $p_n = F_\varepsilon^n(p_0)$ would approach the same saddle fixed point as $n \to -\infty$. Now take a small piece of the unstable manifold around p_0, and map it forward. Poincaré reasoned that the images of this piece under the iteration of F_ε would eventually follow the unstable manifold to come back to intersect the stable manifold again. See Figure 3(a). Likewise, a small piece of stable manifold around p_0 would be mapped backward, eventually following the stable manifold to induce new intersections. Consequently, the stable and unstable manifold would form a web, the structure of which appeared to be incomprehensibly complicated. See Figure 3(b). For solutions in this complicated mesh, which he called a *homoclinic tangle*, dynamical stability appeared unlikely.

We note that, to obtain a homoclinic tangle, one does not need to start with an ordinary differential equation. All it takes is to have a 2D map with a saddle fixed point and to acquire a point of transversal intersection of the stable and unstable manifold of this saddle fixed point. We also note that the original purpose to study homoclinic tangles, historically, was to understand the complicated structures of solutions in the vicinity of an unperturbed homoclinic solution of equation (3.2).

4. Smale's Horseshoe

From the time of Henri Poincaré to the early 1960's, many people, including Birkhoff ([7]), Cartwright and Littlewood ([9]), Levinson ([16]), Sitnikov ([37]) and Alekseev ([1]), had studied many systems of differential equations from celestial mechanics, material science and electric circuits. They had proven rigorously in quite a few of these equations that homoclinic tangle exists. Some had also come to the conclusion that periodic solutions accumulate in homoclinic tangle. Birkhoff and Levinson even used symbolic sequences to code the solutions.

Interestingly enough, the next breakthrough was brought along by Stephen Smale in correcting one wrong conjecture of his own. Smale conjectured that accumulations of periodic orbits are vulnerable to small perturbations. This conjecture, unfortunately, was in direct contradiction to the conclusions of the researches referred to in the last paragraph. In trying to understand the contradiction between his conjecture and these well-established work, Smale realized that there is a rather *simple* geometric structure embedded in *all* homoclinic tangle, and that this structure produces an accumulation of periodic solutions and other complicated dynamical behavior ([34]).

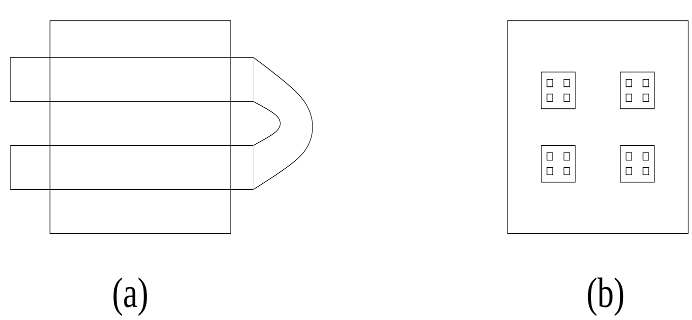

Figure 4. Smale's horseshoe

The geometric structure Smale introduced is as follows. Let us start with a 2D square. We first compress it in the vertical direction and stretch it in the horizontal direction to make a thin and long strip. We then fold the strip and put it back on the original square. See Figure 4(a). This defines a map, which Smale called a *horseshoe map*.

Under the horseshoe map, part of the square is mapped out and part is mapped back into the square. Smale observed that there is a subset that would stay inside of the square forever under the forward and the backward iterations of the horseshoe map, and this set has a complicated but thoroughly understandable structure. A conceptual way to comprehend the structure of this invariant set is to forever replace every square by four smaller squares inside, starting with the original square. See Figure 4(b). It is not hard to show that this invariant subset contains infinitely many periodic orbits of saddle type.

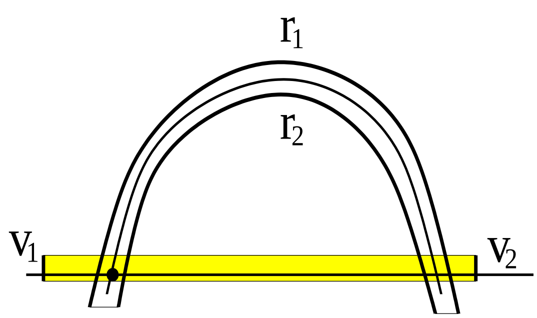

Figure 5. Horseshoe embedded inside of a homoclinic tangle

Smale illustrated that every homoclinic tangle contains a horseshoe. This is shown in Figure 5. Starting with a horizontal strip containing a segment of the stable curve, as drawn in Figure 5. Denote the vertical boundaries of this strip as v_1 and v_2 respectively. Iterating by using the time-T map, the image of v_1 would eventually become the arc labeled as r_1, and v_2 as r_2, in Figure 5. To turn this figure around 90 degrees, we would see Figure 4(a).

The elegance and the simplicity of Smale's construction made a very complicated mathematical situation accessible to even non-mathematicians. Together, with the later discoveries of similar elegance and simplicity, such as the *Lorenz butterfly* ([19]), Li-York's *period three implies chaos* ([17]), and Feigenbaum's *periodic doubling diagram* ([12]), it generated great enthusiasm for the chaos theory in the general scientific community in 1970s and 1980s.

5. Theory on Henon Maps

To define and to study homoclinic tangles, we do not have to start with a differential equation. To induce a homoclinic tangle following Poincaré's observation, all it takes is to have a map with a saddle fixed point and a transversal intersection of its stable and unstable manifold. Maps with homoclinic tangle are easy to come up with and iterating a map is much easier than solving a differential equation. Therefore it was almost like a liberation when the attention was gradually shifted from equation to maps. Questions of independent mathematical interest arose and dynamical systems as a research subject exploded. In this history of fascinating progresses, two maps have commanded tremendous attention: the *Anosov diffeomorphism* ([3]) and the *Henon maps* ([15]).

Anosov diffeomorphism is a map for which the *entire phase space* is one homoclinic tangle. The phase space is the 2D torus $\mathbb{T}^2 = \mathbb{R}^2/\mathbb{Z}^2$, and this map is induced on $\mathbb{T}^2$ by the linear map

$$x_1 = 2x + y, \qquad y_1 = x + y. \tag{5.1}$$

Thanks to the simplicity of (5.1), the dynamic structure of this homoclinic tangle is thoroughly comprehensible. It is nonetheless complicated: The defining matrix of this linear map has two positive eigenvalues; one is > 1 (the unstable eigenvalue) and the other is < 1 (the stable eigenvalue). The eigen-space of the former in $\mathbb{R}^2$ is the unstable manifold of the saddle fixed point $(x, y) = (0, 0)$, and that of the latter is the stable manifold. Both the stable and the unstable manifold of $(0, 0)$ wrap around on the 2D torus as dense curves, and the intersection of these two curves are also dense in the 2D torus. For this map, periodic orbits are also dense on the 2D torus and they are all saddles, each of which has a stable manifold and an unstable manifold wrapping around the 2D torus as dense curves.

All periodic orbits and their stable and unstable manifold, however, are collectively a zero measure set on the 2D torus. Deleting this zero measure set, what remains is still a set of full measure. In this remainder set of full Lebesgue measure, individual orbits behave rather erratically in the sense that they all jump around without any allotted sense of destination. Such disorderly behavior was then characterized and commonly referred to as a *chaos*. It has turned out, however, that in this chaos there exists a *law of statistics* that governs the asymptotic behavior for all: the asymptotic distributions of points of individual orbit in phase space are *the same* for almost all orbits. This governing law of statistics has been commonly referred to as an SRB measure. The theory of SRB measures was independently developed by Sinai ([32]), Ruelle ([31]) and Bowen ([8]) for *uniformly hyperbolic systems*[3], of which Anosov diffeomorphism is a distinguished example.

We end this short discussion on Anosov diffeormophism by noting that chaos and SRB measure presented in Anosov Diffeomorphism are induced exclusively by the non-trivial topology of the 2D torus. The underlining map (5.1) for this homoclinic tangle is linear. Chaos in homoclinic tangles of equation (3.2), on the other hand, are induced into existence by *shearing* in phase space enacted through nonlinear terms in the defining equation. This kind of chaos has been referred to as *shearing induced chaos*. See [46], [18]. Homoclinic tangles represented by Anosov diffeomorphism and that of equation (3.2) are intrinsically different dynamic objects, and consequently, the conclusions of the study of Anosov diffeomorphism and its extension on *uniformly hyperbolic systems* can not be directly applied to homolinic tangle of equation (3.2). With this in mind we now move on to the study of Hénon maps.

Henon maps are a two parameter family of 2D maps in the form of

$$x_1 = 1 - ax^2 + by, \qquad y_1 = bx \tag{5.2}$$

where a, b are parameters and $(x, y) \in \mathbb{R}^2$. This map was introduced by French astronomer Hénon in 1976 as a simple extension of the quadratic family $f(x) = 1 - ax^2$ to 2D. Hénon numerically plotted the possible destinations of individual orbits in a parameter range where homoclinic tangles exist. For some parameters he plotted stable periodic orbits, but for others he plotted messy pictures as shown in Figure 6.

[3] The precise statement for uniformly hyperbolic maps is slightly weaker: the attractive basin of an SRB measure is with a positive Lebesgue measure, not necessarily almost everywhere, in phase space.

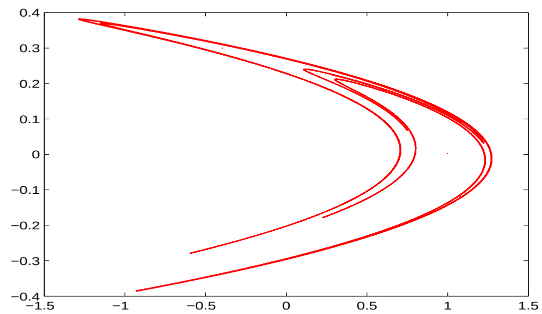

Figure 6. Strange attractors in Hénon maps

It was soon realized that the phenomenon revealed by Hénon occurs commonly for nonlinear maps. For a large class of nonlinear maps, numerical plots of orbits would either end up with a stable periodic orbit, or a messy picture resembling Figure 6. Simulation also illustrated that, for the likes of Figure 6, what was plotted (dropping the initial segment of orbit) was independent of the initial point of the plotting, strongly suggesting the existence of a new type of chaos governed by a law of statistics, that is, an invariant measure that corresponds to the SRB measures for uniformly hyperbolic maps.

Asymptotically stable periodic orbits are natural destinations for other orbits. Their presence in numerical plots are rather expected because, when in existence, open sets of orbits are attracted to them. Here, the issue is on how to justify, in precise terms, what is plotted in Figure 6.

It took a long while for a rigorous dynamics theory to emerge for the strange attractor plotted in Figure 6. With a *tour de force* analysis, Benedicks and Carleson ([4]) asserted that for the Hénon family there is a positive Lesbegue measure set of parameters, for which the corresponding maps admit *no stable periodic orbit*.[4] For maps with no stable periodic orbits, we are in a situation that is somewhat similar to *chaos* in Anosov diffeomorphism: there are no alternatives in phase space to offer an allotted destination, so all orbits would dance around, not knowing eventually where to go. For these maps, we would end up with the plot of Figure 6. We note that it is critically important for the set of parameters of the maps with no stable periodic orbits to have a positive Lebesgue measure in parameter space; it implies that there is a positive probability these maps show up in numerical simulation.

The next step was to understand the dynamics of the object plotted in Figure 6. Equipped with Benedicks-Carleson's technical analysis of the Hénon maps, Benedicks and Young ([6]) proved that, for every "good" Hénon map asserted in [4], there also exists a predestined asymptotic distribution for almost all orbits. This way, the theory of SRB measures was extended to cover "good" Hénon maps. A complete dynamics profile for these maps was also provided later by Young and myself ([43]), with which we acclaimed a comprehensive understanding on the dynamics of the object plotted in Figure 6. It has turned out that, chaos presented in Anosove diffeomorphism is not nearly as complicated as chaos presented in good Hénon maps: The dynamics of the former is a sub-shift of finite type, all orbit of which can be coded by using a finite transition matrix. The latter, though remains a sub-shift, is not of finite type therefore can not be code by using transition matrix.

[4]This statement is a little stronger than what Benedicks and Carleson were able to prove in [4], but they were close enough. The result as stated was first proved by Benedicks and Viana in [5].

6. Homoclinic Tangency and Newhouse Theory

In previous sections, we have introduced two main dynamic objects: the Smale horseshoe and the SRB measure of Benedick-Carleson and Young. Smale's horseshoe is obviously a participating object in homoclinic tangles of equation (3.2), but to identify the SRB measure of Benedicks-Carleson and Young in the homoclinic tangles of equation (3.2) as a participating object we would need to introduce yet another sophisticated dynamics theory. This is the Newhouse theory on homoclinic tangency ([25], [26]). With this theory we will also be able to extend our list of participating dynamic objects for the homoclinic tangles of equation (3.2) to include Newhouse sinks. In Sections 7 and 8, we will rely on the Newhouse theory to prove the existence of SRB measure of Benedick-Carleson and Young inside the homoclinic tangles of equation (3.2).

Newhouse studied a class of one parameter family of maps, in which he replaced the transversal intersection of the two curves in Figure 2(b) in Section 3 by a quadratic tangency. See Figure 7(a). He assumed that the saddle fixed point is *dissipative*, which is to say that the determinant of the Jacobian matrix at the saddle fixed point is with a magnitude < 1. He also assumed that as the parameter varies, the two curves at the point of tangency pass each other. See Figure 7(b).

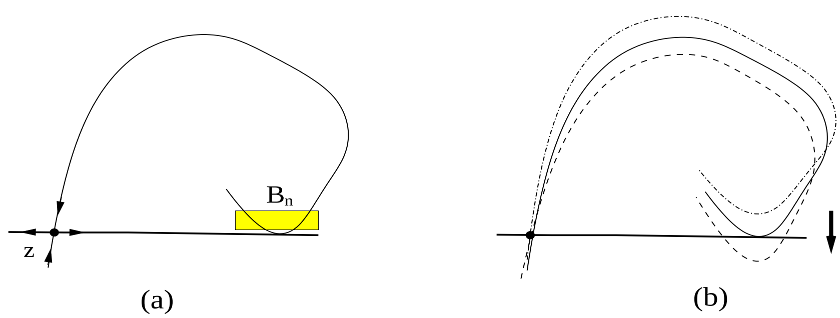

Figure 7. Transversal Homoclinic Tangecy

By assuming that the fixed point is dissipative, Newhouse observed that there is a small rectangular box that would eventually be mapped back into itself (See Figure 7(a)). He re-scaled this box to size $\approx \mathcal{O}(1)$, and discovered that *the renormalized return maps are virtually a Hénon family.*

Based on this fact on the renormalized maps, in particular on the fact that it covers Hénon maps of parameters around b small and $a = 2$, Newhouse then developed a rather sophisticated theory to concluded that (1) there are many other parameters, for which transversal homoclinic tangency exists, and (2) there are also infinitely many parameters for which the corresponding maps have asymptotically stable periodic orbits. Item (1) has been commonly characterized as the *persistency* of the Newhouse tangency, and item (2) has been commonly referred to as Newhouse's *infinite many sinks.*

Newhouse's theory appeared earlier than the theory of Benedicks and Carleson on Hénon maps. With this belated theory, a new dynamic scenario, the dynamics of "good parameters" of Benedicks and Carleson, was added to the Newhouse theory. This addition was first worked out in detail by Mora and Viana ([22]). Combined with the work of Benedick and Young on the existence of SRB measures, it was concluded that, around any given value of parameter of Newhouse tangency, there are three infinite set of parameters, for which the corresponding maps respectively admit (a) Newhouse tangency, (b) asymptotically stable periodic orbits, or (c) SRB measure of Benedicks-Carleson and Young.

7. Infinitely Wrapped Horseshoe Map

Our discussion has moved completely from equations to maps. This is a reflection of a historic trend, in which the study of ordinary differential equations has faded gradually into the background.

As far as the homoclinic tangles of equation (3.2) are concerned, Smale's horseshoe is placed directly in as part of homoclinic tangles for all ε, but Anosov diffeomorphism is not directly relevant. Now how about the relevancy of SRB measures of Benedicks-Carleson and Young and the Newhouse sinks? The answer is that they are both participating dynamic objects in homoclinic tangles of equation (3.2), not for all ε though. SRB measures of Benedicks-Carleson and Young and Newhouse sinks act as competing dynamical scenarios in the space of ε, coexisting always with a horseshoe of infinitely many branches, of which Smale's two-branch horseshoe is a small part.

We present the result of our theory in two steps. The first step is to introduce yet another one parameter family of maps we name as *infinitely wrapped horseshoe maps* and present an overview on the dynamics of the invariant sets of the maps in this family. Through Newhouse tangency, the existence of which can be rigorously confirmed for infinitely wrapped horseshoe maps, we place both SRB measures of Benedick-Carleson and Young and Newhouse sinks in these invariant sets as participating objects. This is done in the current section. The second step is to extend this overview to cover homoclinic tangles of equation (3.2) to bring the study of homoclinic tangles in ordinary differential equations back to the foreground. This is done in Section 8.

Let $\mathcal{A} = \mathbb{S} \times [0,1]$ where $\mathbb{S} = \mathbb{R}/2\pi\mathbb{Z}$ is the unit circle. For $(\theta, y) \in \mathcal{A}$, we let

$$\theta_1 = a + \theta - 10\ln(0.001y + \sin\theta), \qquad y_1 = 0.001\sqrt{0.001y + \sin\theta} \tag{7.1}$$

where $a \in (0, \infty)$. This family of maps, which we denote as $\mathcal{T}_a$, are defined on the part of $\mathcal{A}$ such that

$$0.001y + \sin\theta > 0.$$

The boundary of this domain, defined by

$$0.001y + \sin\theta = 0, \tag{7.2}$$

is two curves. One is 0.001-close to $\theta = 0$, and the other is 0.001-close to $\theta = \pi$ in C^1-norm. They cut $\mathcal{A}$ into two regions that are roughly rectangular in shape. All maps in $\mathcal{T}_a$ are defined on one of the regions, which we denote as D, but not on the other. See Figure 8.

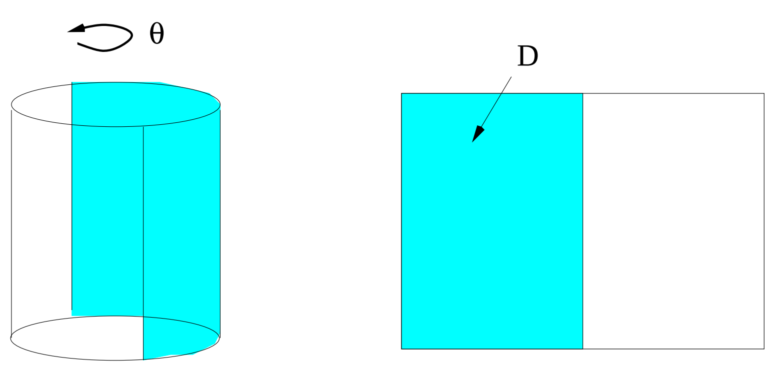

Figure 8. Domain of $\mathcal{T}_a$

The *objective* of our study constitutes *two parts*. The first part is to understand the dynamical structure of the invariant set of $\mathcal{T}_a$ for a fixed value of a. The second part is to understand the way different invariant sets for different values of a are fitted together in parameter space. On certain occasions a complete answer with mathematical rigor is attainable, but on other occasions, we can only extract answers that are partial in nature.

Take the theory on Hénon maps as an example: we know that if (a, b) is a "good" parameter, then the dynamics of the corresponding map is with an SRB measure of Benedick-Carleson and Young. In this case, a comprehensive profile has also been put together to acclaim a thorough understanding of the dynamics of these invariant sets (See [43], [44] and [45]). Now how about around a Newhouse tangency? The information acquired from the Newhouse theory is very insightful, but what we have attained is nevertheless only a partial characterization.

Take Smale's horseshoe as another example. The statement that all homoclinic tangles contain a horseshoe is highly informative but as a complete characterization it is far from sufficient. On the contrary, a statement affirming that a given homoclinic tangle is composed exclusively of a horseshoe would be something completely different in nature: it is a complete characterization.

The point of views stated in the last three paragraphs may be taken as a theoretic standing of point. There is also a way to state our objectives in a less strict fashion, which we regard as *a simulation standing of point*: here we ask what one could expect to plot for a given value of a, and in what way different plots of invariant sets emerge in numerical simulations.

In summary our aims are to understand (a) the dynamics of individual invariant set, and (b) the organization of different invariant sets in parameter space. With both (a) and (b) in mind we now move to present an *overview* on the dynamics of the invariant sets of $\mathcal{T}_a$.

(a) The dynamics of individual invariant set The actions of a map $\mathcal{T}_a$ on D are as follows. First it compresses D in the y-direction, but stretches it in the θ-direction. Because of the logarithmic singularity, this image is stretched to infinite length at the vertical boundaries of D. This infinitely long strip is then folded at $\mathcal{T}_a(\theta, y)$ where $\theta \approx \tan^{-1} 100$ and placed back into $\mathcal{A}$, with the two infinitely long tails wrapping around $\mathcal{A}$ indefinitely. See Figure 9. In this figure the pre-image of the folded part is marked as V, and the folded image is marked as $\mathcal{T}_a(V)$. The dynamics of the invariant set of $\mathcal{T}_a$ are largely determined by *the location of the folded part of the image $\mathcal{T}_a(V)$ in $\mathcal{A}$.*

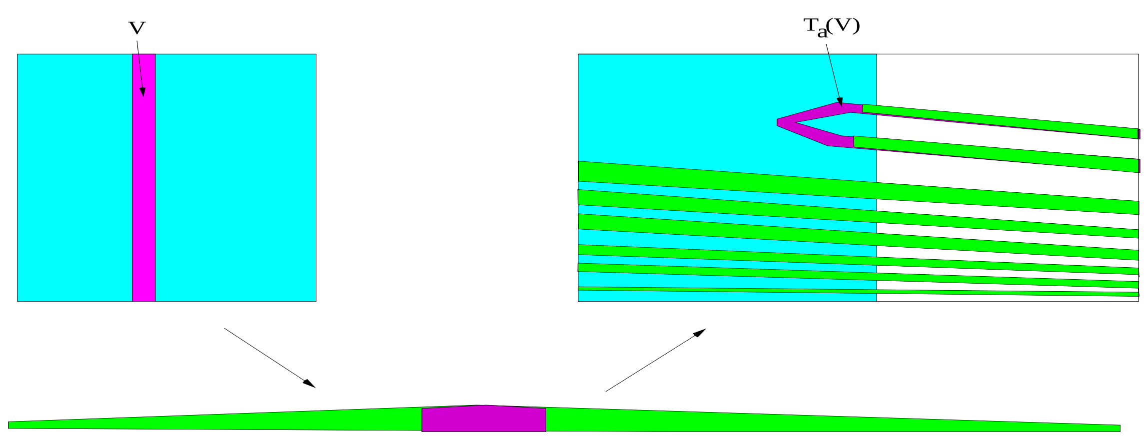

Figure 9. Infinitely Wrapped Horseshoe Map

One obvious conclusion for $\mathcal{T}_a$ is that, for roughly half of the parameters $a \in [0, 2\pi]$, the folded part of the image $\mathcal{T}_a(V)$ is casted out of D. For these parameters the *entire invariant set of $\mathcal{T}_a$ is one horseshoe of infinite many branches*. See Figure 10. In this figure the horizontal strips are $D \cap \mathcal{T}_a(D)$, and the vertical strips are $\mathcal{T}^{-1}(D \cap \mathcal{T}_a(D))$. The structure of a horseshoe of infinite branches is like what was depicted in Figure 4(b) in Section 4, but we need to replace the configuration of 2×2 squares in that figure by using a configuration of $\infty \times \infty$ squares.

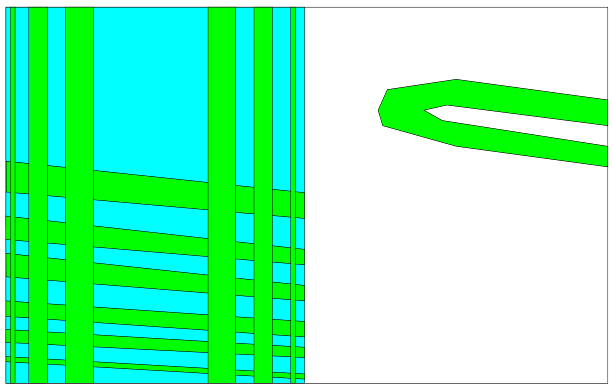

Figure 10. Horseshoe of infinitely many branches

Next we observe that there is an open set of a, for which the images of the folded part $\mathcal{T}_a(V)$ is placed back deep inside of D so that they are sufficiently close to V. For these parameters we have in V a strongly attractive periodic orbit for the corresponding maps. See Figure 11.

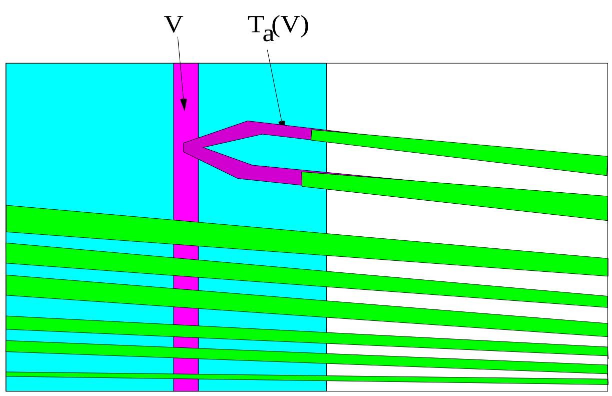

Figure 11. Strongly attractive stable periodic orbit

We can now add all dynamical scenarios associated to Newhouse tangency to this overview. It takes some work to prove the existence of Newhouse tangency for $\mathcal{T}_a$, and this proof goes as follows. First, we observe that a horseshoe of infinitely many branches exists for $\mathcal{T}_a$ for all a thanks to the *infinitely wrapped* nature of $T(D)$ in $\mathcal{A}$. [5] Second, taking a periodic orbit in this horseshoe, we can prove that the unstable manifold of this periodic orbit is a

[5]We note that the presents of this horseshoe of infinitely many branches for all a makes $\mathcal{T}_a$ very different from the *partial horseshoe* characterized by putting the folded part of a Smale horseshoe back inside of its defining domain. For $\mathcal{T}_a$, there is one horseshoe for all a and it is never only partially defined.

roughly horizontal curve in D, which we denote as ℓ_h. We can also prove that the stable manifold of this periodic orbit is a curve cutting vertically across $\mathcal{A}$ in D, which we denote as ℓ_v. The image of ℓ_h is a folded curve, which is dragged by our varying a to pass ℓ_v, inducing Newhouse tangency. See Figure 12.

Consequently, there is a positive measure set of a, so that $\mathcal{T}_a$ contain a strange attractor with an SRB measure of Benedick-Carleson and Young. It also follows from the Newhouse theory that there exists an open set of a so that $\mathcal{T}_a$ has stable periodic solution.

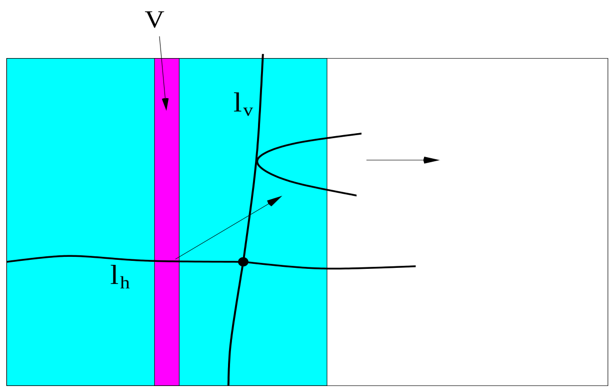

Figure 12. Transversal Homoclinic Tangency

(b) Organizations of invariant sets in parameter space We start with an obvious claim that the dynamics of $\mathcal{T}_a$ is 2π-periodic in a. This is to say that the invariant set defined by $\mathcal{T}_a$ is identical to that of $\mathcal{T}_{a+2\pi n}$ for all n. The second observation is that, as a varies, the images of $\mathcal{T}_a(D)$ is dragged in $\mathcal{A}$ in the θ-direction, and the folded tip is moving at a speed of 1 with respect to a.

When the folded part of $\mathcal{T}_a(D)$ is dragged across the vertical boundaries of D, Newhouse tangency would happen in a way, the details of which are incomprehensibly complicated. Every saddle periodic orbit in that horseshoe of infinitely many branches is with a horizontal unstable manifold that would be mapped back as a folded curve. As a varies, the folded tip would pass the stable manifold of other saddles, all cutting across D as near vertical curves accumulating to the vertical boundaries of D. Sinks and SRB measures, and possibly others yet to be revealed, are all mingled in an exceeding complicated way.

(c) From the simulation standing of point As far as numerical plots are concerned, all the fine details of the impossibly complicated mingling of sinks and SRB measures would be erased by numerical error. We would be left with a dynamical structure of finite precision, in which three dynamical scenarios would likely to show up. They are: *(a) nothing at all; (b) stable periodic orbit; and (c) SRB measure of Benedicks-Carleson and Young.* We note that (a) happens if the folded part of $\mathcal{T}_a(D)$ is mapped out of D. In this case horseshoes do not show up in numerical plots: almost all orbits initiated in D would eventually be plotted out of D.

8. Dynamics of Homoclinic Tangles of Equation (3.2)

In this section we study the differential equation (3.2) assuming $x \in \mathbb{R}^2$. Let $g(x, t)$ be such that

$$g(x, t) = g(x, t + T)$$

for a constant $T > 0$ and for all (x, t). To study equation (3.2), we first introduce an angular variable θ to rewrite it as

$$\frac{dx}{dt} = f(x) + \varepsilon g(x, \omega\theta), \qquad \frac{d\theta}{dt} = \omega^{-1} \tag{8.1}$$

where $\omega = 2\pi T^{-1}$ is the forcing frequency and (x, θ) is in the *extended phase space* $\mathbb{R}^2 \times \mathbb{R}/(2\pi\mathbb{Z})$. Equation (8.1) with a small non-zero ε is commonly referred to as the *perturbed equation*, and when $\varepsilon = 0$ it is referred to as the *unperturbed equation*. We assume $x = 0$ is a saddle fixed point of the unperturbed equation ($\varepsilon = 0$), and it has a homoclinic solution. That is, a solution approaches $x = 0$ in both forward and backward times.

In our study we do *not* use the time-T map to study the homoclinic tangles of equation (8.1). In its stead we use the *separatrix map* introduced by Shilnikov ([35]). To construct the separatrix map, we start with a short segment intersecting the homoclinic solution in the space of x, which we denote as I. We extend I in the direction of θ to form an annulus $\mathcal{A} = \mathbb{S} \times I$ in the extended phase space where $\mathbb{S} = \mathbb{R}/(2\pi\mathbb{Z})$. The separatrix map is the return map that is defined by the solutions of (8.1) from $\mathcal{A}$ back to $\mathcal{A}$. See Figure 13.

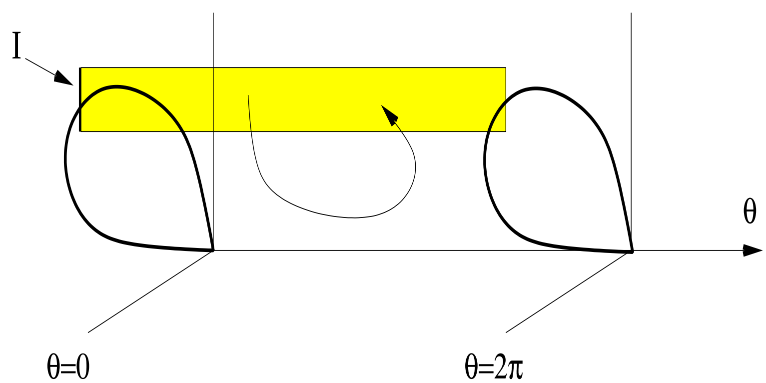

Figure 13. The Separatrix Map

The separatrix map, though not used as extensively as the time-T map in the study of differential equations, has been nevertheless employed as a technical alternative by many. It was the main technical tool in the construction of Shilnikov attractors ([36], [2], [10]). It has also been used as an alternative venues to study the Arnold diffusion in Hamiltonian equation ([27]). What is summarized in the rest of this section is another application of this alternative approach.

Let $x = 0$ be a saddle fixed point of the unperturbed equation in x-space, β be the unstable eigenvalue, and $-\alpha$ be the stable eigenvalue of $x = 0$. We assume $x = 0$ is a *dissipative* saddle. This is to say that we assume

$$\alpha > \beta > 0. \tag{8.2}$$

We also assume that the unperturbed equation has a homoclinic solution.

With these assumptions, Ali Oksasoglu and I computed the separatrix map $\mathcal{R} : \mathcal{A} \to \mathcal{A}$ in [41]. By a simple rescale, which resized I to $[-1, 1]$, we wrote the map $\mathcal{R}$ in terms of $(\theta, y) \in \mathbb{S} \times [-1, 1]$. We attained a formula for $\mathcal{R}$ for equation (8.1).

A major part of the derivation in [41] is to identify terms that do not alter the overall dynamics of $\mathcal{R}$. We caution that these term are not necessarily the usual error terms. Take the infinitely wrapped horseshoe map in the previous section as an example. We can add a large constant to the formula for θ_1 without effecting the overall dynamics of these maps. With all these "secondary terms" removed, what remained for $\mathcal{R}$ is in the form of

$$\begin{aligned} \theta_1 =& \frac{\omega}{\beta}\ln\varepsilon^{-1} + \theta + \frac{\omega}{\beta}\ln(k_0 y + W(\theta)) \\ y_1 =& \varepsilon^{\frac{\alpha}{\beta}-1}(k_0 y + W(\theta))^{\frac{\alpha}{\beta}}. \end{aligned} \tag{8.3}$$

where k_0 is such that $\varepsilon << k_0 << 1$, and $W(\theta)$ is the classical Melnikov function.[6] We also have

$$\frac{\alpha}{\beta} - 1 > 0$$

by assuming $x = 0$ is a dissipative saddle (See (8.2)). This makes the y-direction a strongly contractive direction.

We note that for a completely rigorous presentation we should use, in the place of (8.3), the rather detailed formula for $\mathcal{R}$ derived in [41], though at the end we would reach exactly the same conclusions. In this presentation, we elected to use (8.3) to avoid a technically involved exposition. We refer the reader who is interested in a detailed rigorous mathematical encounter to [41].

We regard the maps in (8.3) as a one parameter family and denote it as $\mathcal{R}_\varepsilon$. We compare $\mathcal{R}_\varepsilon$ with the infinitely wrapped horseshoe maps $\mathcal{T}_a$ in (7.1). Looking at the θ_1 component, we see that the parameter a in $\mathcal{T}_a$ corresponds to

$$a = \frac{\omega}{\beta}\ln\varepsilon^{-1}$$

in $\mathcal{R}_\varepsilon$. However, $\mathcal{R}_\varepsilon$ is *not periodic* in a because ε is also involved in the y_1 component. Instead of a strict periodicity in parameter space, $\mathcal{R}_\varepsilon$ only admits an *asymptotic periodicity* with respect to $\tilde{a}$ as $\varepsilon \to 0$. Conceptually, we can think of $\mathcal{R}_\varepsilon$ as a 2D extension of the 1D family

$$\theta_1 = a + \theta + \frac{\omega}{\beta}\ln(k_0 y + W(\theta))$$

where $a = \frac{\omega}{\beta}\ln\varepsilon^{-1} mod(2\pi)$. The periodicity of the dynamics of $\mathcal{R}_\varepsilon$ in parameter space is embedded asymptotically in this $1D$ family.

Second, the Melnikov function $W(\theta)$ takes the place of the function of $\sin\theta$ in $\mathcal{T}_a$. This is to imply that the curves defined by

$$k_0 y + W(\theta) = 0$$

are the boundaries of the domain of $\mathcal{R}_\varepsilon$. These near vertical curves would cut the annulus $\mathcal{A}$ into roughly rectangular regions. In general, the domain of $\mathcal{R}_\varepsilon$ is now allowed to have more than one rectangular region.

We further observe that the actions of $\mathcal{R}_\varepsilon$ on each of these rectangular regions are similar to the actions of $\mathcal{T}_a$ on D. It compresses it in the y-direction, and stretches it in the θ-direction to infinite length on both side. This image is then folded and place back, with two infinitely long tails wrapping around $\mathcal{A}$ indefinitely. What is new here is that this image may be folded at more than one place depending on the shape of $W(\theta)$.

In summary, homoclinic tangle of equation (8.1) is a one parameter family and ε is the parameter. On a parameter interval $[\varepsilon_1, \varepsilon_2]$ satisfying

$$\frac{\omega}{\beta}\ln\varepsilon_2 - \frac{\omega}{\beta}\ln\varepsilon_1 = 2\pi, \tag{8.4}$$

[6]Explicit formula for $W(\theta)$ was first acquired by Poincaré for a periodically perturbed pendulum to verify the existence of non-tangential intersection of stable and unstable manifold, then for many other equations in later studies (See [13]).

homoclinic tangles fit together in a predestined pattern that mimic what was outlined in the previous section for $\mathcal{T}_a$, $a \in [0, 2\pi]$, and this predestined pattern is repeated indefinitely in an asymptotic fashion as $\varepsilon \to 0$. Note that ω is the forcing frequency and β is the unstable eigenvalue of the fixed point $x = 0$.

Within one period of this repeating pattern, three dynamical scenarios are competing in parameter space. The first is the case in which the entire homoclinic tangle is a horseshoe of infinitely many branches, the second is that of an asymptotically stable periodic orbit; the third is that of an SRB measure of Benedicks-Carleson and Young. This dynamics pattern is exceedingly complicated around the values of ε at which the folded part of the images are dragged crossing the boundary curves of the domain of $\mathcal{R}_\varepsilon$ by our varying ε. On the other hand, in numerical simulations all fine details of this indescribably complicated pattern are expected to be erased by numerical error, and we will end up with a finite alternation of the three aforementioned dynamical scenarios in parameter space.

An Overview: Conceptually, we can regard the homoclinic tangles of second order equation (3.2) as a staged show that is casted around *one* horseshoe of infinitely many branches. Let D be a rectangular region on which the separatrix map $\mathcal{R}_\varepsilon$ is defined. The stage where this show is enacted is D. When the folded part of the image $\mathcal{R}_\varepsilon(D)$ is casted out of D in $\mathcal{A}$, the stage is darkened so this horseshoe is hidden from us in the sense that it is not observable in numerical simulations. When the folded part is dragged passing through D, the elements of this horseshoe are lighted up, **not all at once, but one by one**, through the light shed by Newhouse tangency.

The same staged show is enacted in infinite repetition as $\varepsilon \to 0$.

9. Result of Numerical Simulation

In this section we present a simulation result to confirm what was acclaimed at the end of the last section. We start with a second order equation

$$\frac{d^2x}{dt^2} + (\lambda - \gamma x^2)\frac{dx}{dt} - x + x^2 = 0 \tag{9.1}$$

where $\lambda, \gamma > 0$ are parameters. Let $y = dx/dt$. The point $(x, y) = (0, 0)$ is a dissipative saddle.

The first step of this simulation is to fix $\lambda = 0.5$ to find a value of γ for which $(x, y) = (0, 0)$ admits a homoclinic solution. This value is attained numerically as $\gamma = 0.577028548901$. We add a time-periodic term to equation (9.1) to obtain

$$\frac{d^2x}{dt^2} + (\lambda - \gamma x^2)\frac{dx}{dt} - x + x^2 = \varepsilon \sin 2\pi t. \tag{9.2}$$

The theory presented in the last section acclaims that, for equation (9.2), there is an arrangement of homoclinic tangles, relatively simple around certain values of ε (when the folded part of the image is out of the domain of the separatrix map), but exceedingly complicated around others (associated to Newhouse tangency). As $\varepsilon \to 0$, this arrangement is indefinitely repeated in parameter space ε. The infinitely refined details of this arrangement, on the other hand, would be erased by numerical error in simulation. Consequently, numerical simulation would produce a finite pattern in parameter space, in which three dynamic scenarios would show up in alternation and they are (a) homoclinic tangle that is composed entirely of one horseshoe of infinitely many branches, (b) homoclinic tangles dominated by assymptotically stable periodic orbit, and (c) Homoclinic tangles with SRB measure of Benedicks-Carleson and Young. In what follows we name (a) as *transient tangle*

TABLE 1. Multiplicative periodicity on ε.

$\lambda = 0.5$, $\gamma = 0.577028548901$, $\beta = 0.78077641$, Predicted Multiplicative Period= 2.1831			
ε	Dynamical Behavior	Actual Ratio	Frequency of Occurrence (%)
$1.577 \cdot 10^{-3}$	Transient tangle	–	94.23
$7.774 \cdot 10^{-4}$	Tangle with SRB measure	–	1.61
$7.637 \cdot 10^{-4}$	Tangle with sink	–	4.16
$7.284 \cdot 10^{-4}$	Transient tangle	2.1650	94.28
$3.574 \cdot 10^{-4}$	Tangle with SRB measure	2.1752	3.18
$3.449 \cdot 10^{-4}$	Tangle with sink	2.2143	2.54
$3.349 \cdot 10^{-4}$	Transient tangle	2.1750	94.54
$1.635 \cdot 10^{-4}$	Tangle with SRB measure	2.1859	1.49
$1.608 \cdot 10^{-4}$	Tangle with sink	2.2143	3.97
$1.536 \cdot 10^{-4}$	Transient tangle	2.1803	94.42
$7.505 \cdot 10^{-5}$	Tangle with SRB measure	2.1785	2.37
$7.308 \cdot 10^{-5}$	Tangle with sink	2.2003	3.21
$7.041 \cdot 10^{-5}$	Transient tangle	2.1815	95.00
$3.415 \cdot 10^{-5}$	Tangle with SRB measure	2.1977	1.91
$3.342 \cdot 10^{-5}$	Tangle with sink	2.1867	3.09
$3.224 \cdot 10^{-5}$	Transient tangle	2.1839	94.29
$1.574 \cdot 10^{-5}$	Tangle with SRB measure	2.1696	3.17
$1.504 \cdot 10^{-5}$	Tangle with sink	2.2221	2.54
$1.474 \cdot 10^{-5}$	Transient tangle	2.1872	94.53
$7.190 \cdot 10^{-6}$	Tangle with SRB measure	2.1892	4.00
$6.931 \cdot 10^{-6}$	Tangle with sink	2.1700	1.71
$6.732 \cdot 10^{-6}$	Transient tangle	2.1895	94.28
$3.272 \cdot 10^{-6}$	Tangle with SRB measure	2.1974	3.23
$3.149 \cdot 10^{-6}$	Tangle with sink	2.2010	2.49

because almost all orbits would be mapped out. We name (b) as *tangle with sink*, and (c) as *tangle with SRB measure*.

In [42] we tabulated the occurrence of these tangles. The simulation result is presented in Table 1.

The proper way to read the first two columns of this table is as follows: We start with $\varepsilon = 1.577 \cdot 10^{-3}$. For ε in between $1.577 \cdot 10^{-3}$ and $7.774 \cdot 10^{-4}$, simulation produces transient tangle. At $\varepsilon = 7.774 \cdot 10^{-4}$, tangle with SRB measure occurs in simulation. Then for ε in between $7.774 \cdot 10^{-4}$ and $7.637 \cdot 10^{-4}$, simulation produces tangle with SRB measure, but tangle with sink occurs at $\varepsilon = 7.637 \cdot 10^{-4}$, and so on.

There is clearly a repeated pattern as shown in Table 1. This pattern is anticipated in theory to be 2π-periodic with respect to $a = 2\pi\beta^{-1} \ln \varepsilon$ where β is the unstable eigenvalue of $(x, y) = (0, 0)$. This periodicity in a, reflected in ε, is *multiplicative*: this is to say letting ε_1 and ε_2 be the end points of an ε-interval such that

$$2\pi\beta^{-1} \ln \varepsilon_2 - 2\pi\beta^{-1} \ln \varepsilon_1 = 2\pi,$$

we have

$$\varepsilon_2 = e^{\beta} \varepsilon_1.$$

For equation (9.2) with $\lambda = 0.5$, $\gamma = 0.577028548901$, we have $\beta = 0.78077641$. The number $e^{\beta} = 2.1831$ is the theoretic prediction of the multiplicative period in ε-space.

The third column of Table 1 is the ratio of the ε value three lines above to the current ε value. To check the predicted multiplicative periodicity in parameter space, one compares these values to the predicted multiplicative period 2.1831. The last column of this table is self-explanatory. The low percentage for SRB measures partially explains why, in many numerical simulations of the past, one has to try hard in searching for such chaotic tangles.

In conclusion, results of numerical simulation clearly match the prediction of the theory presented in the last section. We refer the reader to [42] for a technically detailed presentation of this numerical simulation.

Acknowledgment: I would like to first thank my friends, Kening Lu and Zhihong Xia, for their long lasting friendship and support. I am also deeply in debt to my Ph.D. advisor Ken Meyer, my postdoctor mentor and long time collaborator Lai-Sang Young, and Don Saari, for their generous support over the years. Without the help they provided at various stages of my career, I could not possibly have survived academically. Just want to take this opportunity to say that I am very, very grateful.

References

[1] V.M. Alekseev, *Quasiradom Dynamical Systems I, II, III*, Math. USSR Sbornik **5** (1968) 73-128, **6** (1968), 506-560, **7** (1969), 1-43.
[2] V.S. Afraimovich and L.P. Shil'nikov, *The ring principle in problems of interaction between two self-oscillating systems*, PMM Vol **41**(4), (1977), 618-627.
[3] D.V. Anosov, *Geodesic flows on compact manifolds of negative curvature*, Proc. Steklov Inst. Math., **90** (1967) 1-209.
[4] M. Benedicks and L. Carleson, *The dynamics of the Hénon map*, Ann. Math. **133** (1991), 73-169.
[5] M. Benedicks and M. Viana, *Solution of the basin problem for Hénon attractors*, Invent. Math. **143** (2001), 375-434.
[6] M. Benedicks and L.-S. Young, *Sinai-Ruelle-Bowen measures for certain Hénon maps*, Invent. Math. **112** (1993). 541-576.
[7] G.D. Birkhoff, *Nouvelles Recherches sur les systemes dynamiques* Mem. Pont. Acad.Sci. Novi Lyncaei, **1**, 85-216 (1935), in particular, Chapter IV.
[8] R. Bowen, *Periodic points and measures for Axiom A diffeomorphisms*, TAMS (1971), 377-397.
[9] K.L. Cartwright and J.E. Littlewood, *On non-linear differential equations of the second order, I: The equation $\ddot{y} + k(1-y^2)\dot{y} + y = b\lambda k \cos(\lambda t + a), k$ large*, J. London. Math. Soc. **20**, (1945), 180-189.
[10] B. Deng, *On Shilnikovs homoclinic saddle-focus theorem*, JDE 102 (1993) 305329.
[11] G. Duffing, *Erzwungene Schwingungen bei Veranderlicher Eigenfrequenz*, F. Wieweg u. Sohn: Braunschweig. (1918).
[12] M.J. Feigenbaum, *Quantitative universality for a class of non-linear transformations*, J. stat. Phys., **19** (1978) 25-52.
[13] J. Guckenheimer and P. Holmes, *nonlinear osscilations, dynamical systems and birfurcation of vector fields*, Springer-Verlag, Appl. Math. Sciences **42** (1983).
[14] D. Florin and P. Holmes, *Celestial encounters: the origins of chaos and stability*, Princeton University Press, Princeton, 1999.
[15] M. Hénon, *A two-dimensional mapping with a strange attractor*, Comm. Math. Phys. **50** (1976), 69-77.
[16] N. Levinson, *A Second-order differential equaton with singular solutions*, Ann. Math. **50** (1949), 127-153.
[17] T.Y. Li and J.A. York, *Periodic three implies chaos*, Amer. Math. Monthly, **82** (1975) 985-992.
[18] K. Lin and L.-S. Young, *Shear-induced chaos*, Nonlinearity **21** (2008) 899-922.
[19] E. N. Lorenz, *Deterministic non-periodic flow*, J.Amer. Sci., **20** (1963), 130-141.
[20] R. McGehee, *Triple collision in collinear three-body problem.* Inventione Mathematicae, **27** (1974), 191-227.
[21] V.K. Melnikov, *on the stability of the center for time periodic perturbations*, Trans. Moscow Math. Soc., **12** (1963), 1-57.
[22] L. Mora and M. Viana, *Abundance of strange attractors*, Acta. Math. **171** (1993), 1-71.

[23] J.K. Moser, *Stable and random motions in dynsmical systems (with special emphasis on celestial mechanics)*, Princeton University Press, Princeton, NJ, (1973).
[24] F. Moulton, *Henri Poincaré*, Popular Astrnomy, **10** (1992), 625.
[25] S. E. Newhouse, *Diffeomorphisms with infinitely many sinks*, Topology, **13** (1974), 9-18.
[26] J. Palis and F. Takens, *Hyperbolicity & sensitive chaotic dynamics at homoclinic bifurcations*, Cambridge studies in advanced mathematics, **35** Cambridge University Press, Cambridge, (1993)
[27] G.N. Piftankin, D.V. Treschev, *Separatrix maps in Hamiltonian systems*, Russian Math. Surveys 62 (2) (2007) 219322.
[28] H. Poincaré, *Mémoire sur les courbes définies par une équation différetielle*, Journal de Mathematiques, **7** (1881), 375-422, and **8** (1882),251-296.
[29] H. Poincaré, *Sur le probléme des trios corps et les équations de la dynamique*, Acta Mathematica, **13** (1890), 1-270.
[30] H. Poincaré, *Les Méthodes Nouvelles de la Mécanique Céleste*, 3 Vols. Gauthier-Villars: Paris (1899)
[31] D. Ruelle, *Ergodic theory of differentiable dynamical systems*, Publ. Math., Inst. Hautes Étud. Sci. **50** (1979), 27-58.
[32] Y. G. Sinai, *Gibbs measure in ergodic theory*, Russian Math. Surveys **27** (1972), 21-69.
[33] C. L. Siegel and J. K. Moser *Lecture on celestial mechanics*, Springer-Verlag, 1971.
[34] S. Smale, *Diffeomorphisms with many periodic points*, Differential and Combinatorial Topology (A Symposium in Honor of Marston Morse), Princeton University Press, (1965), 63-80.
[35] L.P. Shilnikov, *A case of the existence of a countable number of periodic motion*, Sov. Math. Dokl. 6 (1965) 163166.
[36] L. P. Shilnikov, *On a Poincaré-Birkhoff Problem*, Math USSR-sb. 3 (1967), 353-371.
[37] K. Sitnikov, *existence of oscillating motions for the three-body problem*, Dokl. Akad. Nauk, USSR, **133**(2), (1960), 303-306.
[38] K. Sundman. *Recherches sur le problème des trois corps*, Acta, Mathematica, 36 (1912) 105-179.
[39] van der Pol B. and van der Mark J., *Frequency demultiplication*, Nature **120** (1927), 363-364.
[40] Q.D. Wang. *The Global Solution of N-body Problem*, Celest. Mech. 50, (1991) 73-88.
[41] Q.D. Wang and A. Oksasoglu, *Dynamics of Homoclinic Tangles in Periodically Perturbed Second Order Equations*, JDE 250(2011) 710-751.
[42] Q.D. Wang and A. Oksasoglu, *Periodic Occurrence of Dynamical Behavior of Homoclinic Tangles*, Physica D: Nonlinear Phenomena 239(7) (2010), 387-395.
[43] Q.D. Wang and L.-S. Young, *Strange attractors with one direction of instability*, Commun. Math. Phys., **218** (2001), 1-97.
[44] Q.D. Wang and L.-S. Young *Toward a Theory of Rank One Attractors*, Annals. Math. 167 (2008), 349-480.
[45] Q.D. Wang and L.-S. Young *Dynamical Profile of a Class of Rank One Attractors*, Ergodic Theory and Dynamical Systems 33(4) (2013) 1221-1264.
[46] Q.D. Wang and L.-S. Young *Strange attractors in periodically-kicked limit cycles and Hopf bifurcations*, Commun. Math. Phys. **24** (2003), 509-529.
[47] Z.H. Xia *The existence of noncollision singularities in the N-body problem*, Annals of Mathematics, **135** (1992), 411-468.